DOI: 10.1534/genetics.107.071225

The Bro1-Domain Protein, EGO-2, Promotes Notch Signaling in *Caenorhabditis elegans*

Ying Liu and Eleanor M. Maine[1]

Department of Biology, Syracuse University, Syracuse, New York 13244

Manuscript received January 24, 2007
Accepted for publication June 2, 2007

ABSTRACT

In *Caenorhabditis elegans*, as in other animals, Notch-type signaling mediates numerous inductive events during development. The mechanism of Notch-type signaling involves proteolytic cleavage of the receptor and subsequent transport of the receptor intracellular domain to the nucleus, where it acts as a transcriptional regulator. Notch-type signaling activity is modulated by post-translational modifications and endocytosis of ligand and receptor. We previously identified the *ego-2* (**e**nhancer of ***glp-1***) gene as a positive regulator of germline proliferation that interacts genetically with the GLP-1/Notch signaling pathway in the germline. Here, we show that *ego-2* positively regulates signaling in various tissues via both GLP-1 and the second *C. elegans* Notch-type receptor, LIN-12. *ego-2* activity also promotes aspects of development not known to require GLP-1 or LIN-12. The EGO-2 protein contains a Bro1 domain, which is known in other systems to localize to certain endosomal compartments. EGO-2 activity in the soma promotes GLP-1 signaling in the germline, consistent with a role for EGO-2 in production of active ligand. Another *C. elegans* Bro1-domain protein, ALX-1, is known to interact physically with LIN-12/Notch. We document a complex phenotypic interaction between *ego-2* and *alx-1*, consistent with their relationship being antagonistic with respect to some developmental processes and agonistic with respect to others.

CELL–CELL signaling is essential for the regulation of developmental decisions in multicellular organisms. Notch-type signaling has been implicated in developmental decisions in diverse animal species and often regulates the proliferation *vs.* differentiation decision (Weinmaster and Kopan 2006; Wilson and Radtke 2006). In *Caenorhabditis elegans*, Notch-type signaling mediates numerous inductive events during embryonic and larval development and in the adult gonad (Greenwald 2005). *C. elegans* has two Notch-type receptors, GLP-1 and LIN-12; they are partially redundant for function in the embryo, but have separate roles in older animals. GLP-1 functions in numerous inductive events in the early embryo (Priess 2005), and GLP-1 signaling in the larva and adult maintains proliferation of the developing germline (Kimble and Crittenden 2005). LIN-12 functions in several cell–cell interactions in the embryo (redundantly with GLP-1) and larvae; its role has been most closely studied in the developing vulva, where it is required for several distinct inductive events (Greenwald 2005).

The canonical Notch pathway has been elucidated by studies in Drosophila and mammals, as well as in *C. elegans*. A transmembrane Delta/Serrate/LAG-2 (DSL) family ligand produced by the signaling cell(s) binds the transmembrane Notch-type receptor in the receiving cell(s) (see Ehebauer *et al.* 2006). Upon ligand-receptor binding, two cleavage events, called S2 and S3, release the extracellular and intracellular domains of the receptor, respectively. The intracellular domain is transported to the nucleus where it interacts with CBF1/Su(H)/LAG-1 (CSL) family transcriptional regulators and other proteins to form a transcriptional activation complex. Signaling pathway activity is modulated in numerous ways, including by post-translational modifications and endocytosis of pathway components in both the signaling and the receiving cell (Schweisguth 2004).

Germline proliferation in *C. elegans* depends on inductive signals from the somatic gonad that are mediated by GLP-1/Notch. The germline begins to proliferate in early larval development in response to signals from the somatic gonad (Greenwald 2005; Kimble and Crittenden 2005). In mid-larval development, proximal germ cells enter meiosis, and proliferation is maintained only in the distal germline. At this time, the somatic distal tip cell (DTC) becomes the sole source of signal; the major DSL-type ligand produced by the DTC is LAG-2. Upon ligand binding, the GLP-1 intracellular domain is thought to be released and transported to the nucleus where it interacts with the CSL-type transcription factor, LAG-1, and an adaptor protein, SEL-8/LAG-3, to activate transcription of target genes (Greenwald 2005; Kimble and Crittenden 2005). When signaling

[1]*Corresponding author:* Department of Biology, Syracuse University, 108 College Place, Syracuse, NY 13244. E-mail: emmaine@syr.edu

is compromised by ablation of somatic signaling cells or mutation in a GLP-1/Notch pathway component, germ cells prematurely exit mitosis, enter meiosis, and differentiate (Kimble and Crittenden 2005; Hansen and Schedl 2006).

To identify factors that regulate Notch-type signaling in the gonad, our laboratory previously recovered *ego* (**e**nhancer of ***glp-1***) mutations that enhanced the germline phenotype of a weak *glp-1* loss-of-function mutation (Qiao *et al.* 1995; J. Spoerke, P. Shu and E. Maine, unpublished data). A single *ego-2* mutation, *om33*, was isolated in that study. Here, we report a molecular and genetic analysis of *ego-2*. We show that *ego-2* encodes a Bro1-domain protein whose activity promotes GLP-1/Notch signaling in the gonad and embryo, and LIN-12/Notch signaling in the AC–ventral uterine (VU) decision. We find that *ego-2* activity in the soma promotes GLP-1 signaling in the germline, suggesting that EGO-2 may promote the production of active ligand. We also show that *ego-2* activity promotes spermatogenesis and several aspects of somatic development not known to require Notch-type signaling. The *C. elegans* genome contains a second Bro1-domain-encoding gene, *alx-1* (Alix-like). We describe a complex genetic relationship between *ego-2* and *alx-1*, which suggests that the EGO-2 and ALX-1 proteins may promote some common aspects of development and act in opposition to regulate others. Bro1-domain proteins in a variety of organisms have been shown to localize to endosomal compartments (Odorizzi 2006). We hypothesize that EGO-2 may participate in endosomal-based processes that modulate Notch-type signaling.

MATERIALS AND METHODS

Nematode strains and culture: Standard culture conditions were used (Epstein and Shakes 1995). Wild-type strains *C. elegans* variant Bristol (N2) and CB4856 ("HA8") and mutations used are as described by Chen *et al.* (2003), as listed in Wormbase (http://www.wormbase.org), or as described in the text. Mutations used were the following: linkage group (LG) I—*ego-2(om33)*, *ego-2(tm2272)*, *fog-1(q253ts)*, *gld-1(q485)*, *gld-2(q497)*, *rrf-1(pk1417)*, *unc-75(e950)*, *hIn1[unc-54(h1040)]*, *hDf17*, *ccIs4251*; LGII—*rrf-3(pk1426)*; LGIII—*alx-1(gk412)*, *dpy-17(e164)*, *glp-1(ar202)*, *glp-1(bn18ts)*, *glp-1(e2142ts)*, *glp-1(oz112gf)*, *lin-11(n389)*, *lin-12(ar170)*, *lin-12(n302gf)*, *unc-32(e189)*, *unc-36(e251)*, *hT2[bli-4(e937) let-?(q782) qIs48] (I;III)*. A *cdh-3::gfp* transgene was used as a marker for the anchor cell (AC) (Inoue *et al.* 2002). ACs were identified by comparing the differential interference contrast and CDH-3::GFP fluorescence images at high magnification (×400, ×630). The phenotype was scored early in vulva formation, prior to the time when CDH-3 expression becomes visible in the vulval precursor cell descendants (see Inoue *et al.* 2002). To test for suppression of a weak *lin-12(gf)* phenotype, we constructed the following stock: *dpy-17 lin-12(n302)/hT2 gfp; cdh-3::gfp*.

The DAPI-staining method and brood size determinations were as described (Qiao *et al.* 1995). To generate *ego-2* mutant males, several sets of ~30 L4 *ego-2(om33) unc-75* hermaphrodites were picked to fresh plates and placed at 30° for ~2 hr; plates were then moved to 20°. L4 *ego-2(om33) unc-75* males were picked from the F_1 generation and mated with *ego-2(om33) unc-75/ego-2(tm2272)* hermaphrodites at 25° to obtain *ego-2(om33) unc-75/ego-2(tm2272)* males. *ego-2* males were tested for a spermatogenesis defect by mating them with *fog-1(q253ts)* XX females at a ratio of 1 female:5 males. N2 males were mated with *fog-1(ts)* females as a control. *ego-2 unc75*, *ego-2 unc-75;alx-1*, and *unc-75* hermaphrodites were mated with N2 males at 25° at a ratio of 1:3. Parents were transferred daily until no additional embryos were laid onto the plates. Some matings were also set up at ratios of 1:1, 1:2, or 1:4 hermaphrodites to males. Within this range, we noted that the number of males inversely correlated with brood size of *ego-2 unc-75* and *ego-2 unc75; alx-1* hermaphrodites. We attribute this effect to the *unc-75* marker, which weakens the hermaphrodites.

Recovery and analysis of deletion allele: The National Bioresource Project recovered a deletion allele lacking the first three predicted exons of Y53H1C.2, called *tm2272*. To balance *tm2272*, we crossed *unc-75/+* males into individual hermaphrodite progeny of a *tm2272/+* mother, recovered cross progeny that segregated *unc-75*, and amplified the DNA to identify lines carrying the *tm2272* deletion. We identified several *tm2272/unc-75* lines, each of which segregated progeny that died as embryos and young larvae. After the *tm2272* was outcrossed a total of five times and balanced with *hIn1*, the lethal phenotype was still associated with the *tm2272* chromosome. DNA from individual arrested larvae was amplified by standard methods; 9/9 animals carried the *tm2272* deletion and did not carry an *ego-2(+)* allele. We conclude that the developmental arrest/lethality is caused by or linked to the *tm2272* deletion allele. *tm2272* failed to complement *om33* for the Ego and spermatogenesis-defective (Spe) phenotypes.

Dosage studies: *ego-2(−)/hDf17* animals were generated as follows. (i) *ego-2(om33) unc-75* hermaphrodites were mated with N2 males, and *ego-2(om33) unc-75/++* F_1 males were mated with *hDf17/hIn1[unc-54]* hermaphrodites. NonUnc hermaphrodites were picked to single plates and cultured at 25°. A subset were Spe; they were stained with DAPI and their morphology was compared with that of *ego-2(om33) unc-75* animals raised at 25°. Non-Spe animals included *ego-2(om33) unc-75/hIn1[unc-54]* (segregated Unc-75 and Unc-54 progeny), *++/hIn1[unc-54]* (segregated Unc-54 progeny), *++/hDf17* (segregated dead embryos), and self-progeny. (ii) *ego-2(tm2272)/hIn1[unc-54]* hermaphrodites were mated with N2 males; *ego-2(tm2272/+)* and *hIn1/+* F_1 males were mated with *hDf17/hIn1[unc-54]* hermaphrodites. The surviving progeny of six matings were scored as Unc or nonUnc. A total of 50 nonUnc hermaphrodites were picked to single plates and scored for a Spe phenotype; none were Spe. If all cross-progeny genotypes were viable, we expected 1/8 (12.5%) to be Unc-54. If *hDf17/ego-2(tm2272)* were inviable, we expected 1/7 (14.2%) of surviving cross progeny to be Unc-54. We observed 16.6% Unc-54 males, suggesting that the *hDf17/ego-2(tm2272)* males are inviable ($n = 1254$ males). (We report the figure for males because nearly all should be cross progeny.) This result is consistent with the failure to recover Spe hermaphrodite cross progeny. The genotypes of the 50 F_1 nonUnc hermaphrodites (based on the phenotypes of their progeny) were the following: 40% *hIn1[unc54]/+* (segregated Unc-54); 24% *hDf17/+* (segregated dead embryos); and 36% *hIn1[unc54]/hDf17* or *hIn1[unc-54]/ego-2(tm2272)* (segregated dead embryos and Unc-54). A subset of the final category segregated arrested *ego-2(tm2272)* larvae well as dead embryos.

Single nucleotide polymorphism mapping: We mapped *ego-2(om33)* relative to single nucleotide polymorphisms, using a strategy similar to that described in Maine *et al.* (2004). We made *lin-11 ego-2(om33)*/HA8;*glp-1(bn18ts)* and *ego-2(om33) unc-75*/HA8*; glp-1(bn18ts)* strains, where HA8 designates a chromosome from the polymorphic CB4856 strain. The *ego-2*,

unc-75, and *glp-1* mutations were generated in a N2 wild-type background. We recovered *lin-11* non-Ego and *unc-75* non-Ego recombinants [on the basis of the absence of an enhanced *glp-1(ts)* phenotype], generated homozygous recombinant lines, and assayed their DNA sequence at a series of polymorphic sites (Figure 1A). Genomic DNA from each recombinant line was amplified (at 95° for 1 min; 30 cycles of 94° for 30 sec, 55° for 30 sec, 70° for 2 min; 70° for 5 min), digested with an appropriate restriction enzyme, and analyzed by agarose gel electrophoresis to determine whether it had N2 or CB4856 sequence at the polymorphic site.

RNA interference assays: RNA interference assay (RNAi) was performed by the feeding method of Timmons *et al.* (2001). For this analysis, we used constructs containing a portion of genomic DNA or cDNA for each of the 21 predicted genes within the 137-kb region. Genomic DNA corresponded to predicted coding regions. DNA fragments were cloned into the L4440 vector to generate "feeding" constructs and transformed into *Escherichia coli* strain HT115 (Timmons *et al.* 2001). *E. coli* strains were grown overnight in liquid culture, seeded onto NGM-Lite plates (Sun and Lambie 1997) that contained appropriate concentrations of ampicillin and IPTG, and allowed to grow at room temperature (~20°–22°) for ~48 hr. Seeded plates were stored at 15° and used within ~2 weeks of seeding. To ensure consistent expression of the double-stranded (ds)RNA, the plasmid was routinely retransformed into HT115. L4 larvae were placed onto the plates at 20°; their progeny were raised continuously in the presence of the dsRNA.

Three Y53H1C.2 "feeding" constructs were generated. The partial 3′ cDNA, yk1162g8, and two genomic DNA regions ("a" and "b" in Figure 1C) were used as inserts. We also performed *ego-2* RNAi in an enhanced RNAi background using *rrf-3(0)*; we observed defects consistent with *ego-2* function in many tissues, as previously reported by Rual *et al.* (2004). Two differences were observed between our data and those of Rual *et al.* (2004), probably reflecting the different RNAi protocols used in the two studies. Rual *et al.* (2004) reported a blistered cuticle defect that we did not observe, and they did not report a coordination defect that we observed.

To test the RNAi sensitivity of *alx-1(0)* mutants, we generated a *ccIs4251; alx-1(0)* strain and a *gfp* "feeding" construct. *ccIs4251; alx-1(0)* and *ccIs4251;alx-1(+)* were placed on the *gfp* feeding strain in parallel, and expression of the GFP-tagged transgenic protein was evaluated.

cDNA analysis: Sequence analysis indicated that yk1162g08 includes the 3′-end of the *ego-2* transcript, since it contains a poly(A) addition sequence (TATAAA) and a terminal poly(A) sequence. We performed reverse transcriptase DNA amplification reactions to obtain the 5′ portion of the cDNA, as follows. Total RNA was extracted from mixed-stage hermaphrodites using Trizol reagent (Invitrogen, Carlsbad, CA) as described by the manufacturer. First-strand cDNA was prepared with SuperScript reverse transcriptase (Invitrogen) using an oligomeric primer corresponding to a sequence in yk1162g08. Amplification reactions were performed under the following conditions: 95° for 1 min; 30 cycles of 94° for 30 sec, 55° for 30 sec, 70° for 2 min; and 70° for 5 min. The oligonucleotide primer used for the reverse transcription reaction corresponded to a sequence in yk1162g08 and is referred to as "Exon10for" (5′-TAGGAAGCTTGAGGTGGTGTG-3′). Reverse transcriptase product was amplified with pairs of oligonucleotide primers corresponding to sequences located within regions "a" and "b" used in the *glp-1* enhancement assays and located within Genefinder-predicted exons (see Figure 1). Pairs of primers used to perform DNA amplification reactions were as follows: Exon10for + Exon9rev (5′-AATACGAGAA GCGTGTCTCGG-3′); Exon10for + Exon8rev (5′-AACGTCG AAAGCTCGTCGAAC-3′); Exon9for (5′-GCTCTTCCATCGC ATGAACCG-3′) + Exon7rev (5′-GAAACGCGGAAAAAGAGA ACG-3′); Exon7for (5′-CTCATCTCTCCCTGCTGCTCC-3′) + Exon123rev (5′-GGAGGCTCTTCCAATAATGC-3′). The prominent amplification product obtained with each primer pair was cloned into pGEM-T vector (Promega, Madison, WI) and sequenced. There was extensive overlap between products from the exon 7–10 region, giving two- to threefold coverage of most of the sequence; we obtained single-fold coverage of exons 11–15 and 1–6. A portion of the 5′-UTR was obtained from a cDNA library (a kind gift from B. Barstead). The cDNA sequence was deposited in GenBank, accession no. EF378622.

We used quantitative RT–PCR to examine *ego-2* mRNA levels in the germline *vs.* soma. We extracted total RNA by the Trizol method (above) from 50 wild-type (N2) and *glp-4(bn2ts)* mutant adults raised at restrictive temperature; the latter have very few germ cells (Beanan and Strom 1992). RNA was dissolved into 50 μl DEPC-treated H_2O. A total of 1, 2, and 5 μl of RNA (*i.e.*, from one, two, and five worms, respectively) was used as template in a 10-μl reverse transcriptase reaction, as described above. The entire reaction was used as template in DNA amplification reactions. Reactions were performed using oligonucleotide primers that flanked an intron, so that any amplification of genomic DNA (if present as a contaminant in the RNA preparation) would be detected; the only visible amplification products corresponded to spliced template.

RESULTS

***ego-2* encodes a Bro1-domain protein:** Qiao *et al.* (1995) mapped *ego-2* between *dpy-24* and *unc-101* on the right arm of chromosome I. We further mapped *ego-2* relative to marker genes and single nucleotide polymorphisms (SNPs) in the region (see materials and methods). By this strategy, *ego-2* was localized to a 137-kb interval that was predicted to contain 21 genes (Figure 1B). We next used RNAi to deplete each of the 21 predicted gene products and tested for enhancement of the *glp-1(bn18ts)* phenotype in the germline (see materials and methods). This assay identified one predicted gene, Y53H1C.2, as an *ego* gene. Approximately 45% of *glp-1(bn18ts)* animals treated with Y53H1C.1 RNAi developed a Glp-1 sterile defect, where all germ cells prematurely entered meiosis during larval development and differentiated as sperm (Table 1; Figure 2D). In contrast, *glp-1(ts)* was not enhanced to sterility by RNAi with any of the other 20 predicted genes. We concluded that Y53H1C.2 was an *ego* gene and tentatively identified it as *ego-2*.

At this time, only a partial (3′) cDNA, called yk1162g08, was available for Y53H1C.2 (kindly provided by Y. Kohara and colleagues, http://nematode.lab.nig.ac.jp) (see Figure 1). To determine the gene structure, we first used the *glp-1* enhancement assay to delineate the approximate size of the Y53H1C.2 coding region. Our original *glp-1* enhancement test was carried out with yk1162g08 as the insert in a "feeding" construct used to generate dsRNA. We generated two additional feeding constructs containing upstream genomic DNA as inserts, referred to as "a" and "b" in Figure 1C (see materials and methods) The *glp-1(bn18ts)* germline

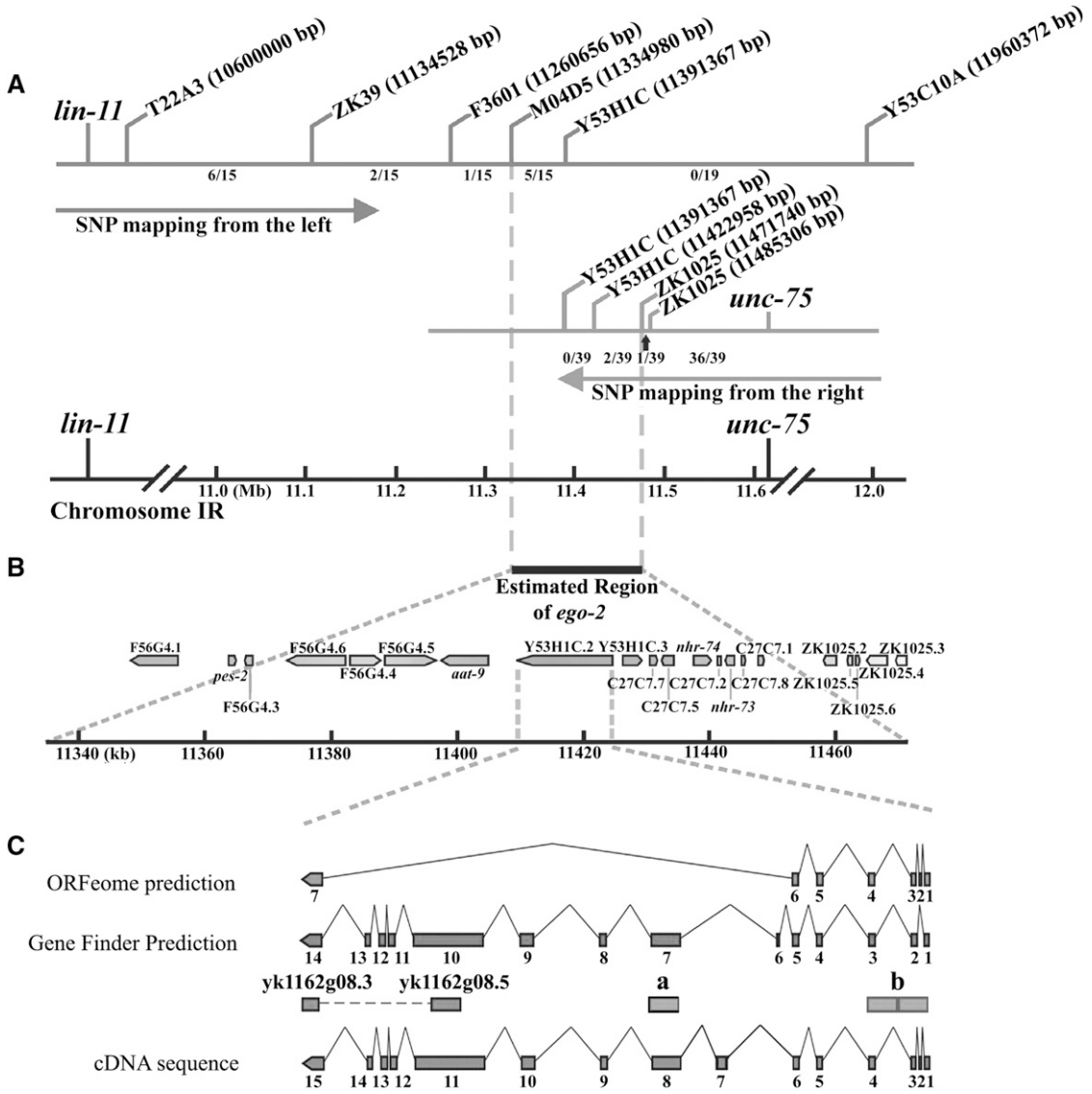

FIGURE 1.—Identification of the *ego-2* gene. (A) *ego-2* was localized to a 137-kb region by mapping relative to SNPs. Relative positions of SNPs are shown; the cosmid or yeast artificial chromosome names and chromosomal coordinates of the SNPs are listed. *lin-11* non-*ego-2(om33)* recombinants were used to determine the left boundary of the *ego-2* region, and *unc-75* non-*ego-2* recombinants were used to determine the right boundary of the *ego-2* region. The number of recombinants recovered within each interval is indicated. (B) Relative locations of the 21 predicted genes in the *ego-2* region. (C) Genefinder and ORFeome gene models for Y53H1C.2 are compared with the cDNA sequence that we obtained. Exons are numbered. The corresponding partial cDNA, yk1162g08.2, is indicated. Yk1162g08.2 was previously sequenced at the ends (boxes), but not within the central region (dashed line). We generated dsRNA feeding clones with yk1162g08.2 and genomic DNA corresponding to fragments "a" and "b" as inserts in the plasmid vector (see MATERIALS AND METHODS).

phenotype was enhanced by RNAi with each of these additional constructs, indicating that Y53H1C.2 extended across this ~15-kb region.

We next obtained the complete cDNA sequence by using yk1162g08 as a starting point for reverse-transcriptase DNA amplification (see MATERIALS AND METHODS). The resulting cDNA sequence contains a 4476-nucleotide open reading frame (Figures 1C and 3A). The predicted product is a 1492-amino-acid protein with a Bro1 domain (Figure 3B). The gene structure revealed by our analysis is different from previously predicted gene models, although it more closely resembles the Genefinder prediction (see Figure 1C). Interestingly, the *C. briggsae* database contains an annotated gene, CBG04380, whose predicted product aligns well with EGO-2 throughout its entirety (BLAST *E*-value = 0) and is presumably an ortholog.

Once we determined the Y53H1C.2 cDNA sequence, we sequenced genomic DNA corresponding to the exons and exon/intron junctions in the *ego-2(om33) unc75* strain (see MATERIALS AND METHODS). We detected a T-to-A substitution at nucleotide 350 in the

TABLE 1

The loss of *ego-2* function enhances *glp-1(bn18ts)* in the germline

Genotype	Adults/brood (*N*)	% Glp-1 sterile (*n*)
glp-1(bn18ts)	191 ± 11 (5)	1.4 (957)
unc-75	190 ± 10 (6)	0 (1138)
ego-2(om33) unc-75	192 ± 11 (6)	0 (1149)
unc-75; glp-1(bn18)	135 ± 3 (12)	0.1 (1620)
ego-2(om33) unc75; glp-1(bn18)	90 ± 12 (10)	8.5 (896)
ego-2(om33/tm2272)	28 ± 3 (14)	0 (398)
ego-2(om33/tm2272); glp-1(bn18)[a]	ND	88 (175)
ego-2(RNAi)[b]	190 ± 8 (12)	0 (2277)
ego-2(RNAi);unc-32 glp-1(bn18ts)[b,c]	134 ± 7 (31)	45 (4160)

Experiments were done at 20°. *N*, number of broods scored; *n*, number of animals scored; ND, not determined. "Glp-1 sterile" is the percentage of germlines in which all germ cells had prematurely exited mitosis, entered meiosis, and differentiated. Number following the "±" is the standard error of the mean.

[a] Animals were obtained as progeny of *ego-2(om33) unc-75/ego-2(tm2272); glp-1(bn18/+)* mothers (whose average brood size was 36 ± 4.5). A total of 321 progeny (nine broods) were scored; 47/214 *ego-2(om33) unc-75/ego-2(tm2272)* animals were Glp-1 sterile, which is 88% (47/53) of the expected number of *glp-1(bn18/bn18)* animals. In addition, 8/107 *ego-2(om33) unc-75* animals were Glp-1 sterile, which is 30% (8/27) of the expected number of *glp-1(bn18/bn18)* animals.

[b] Data are the average of four independent feeding experiments.

[c] A similar degree of enhancement was observed in the absence of the *unc-32* marker (data not shown).

protein-coding region that is not present in the parental *unc-32(e189) glp-1(bn18ts)* strain (Figure 3, A and B). This mutation is predicted to cause a valine-to-glutamine substitution at amino acid 117, a semiconserved residue within the Bro1 domain (Figure 3, A and B). After we identified the *om33* lesion, S. Mitani and colleagues recovered a partial deletion within the *ego-2*/Y53H1C.2 gene region, called *tm2272* (National Bioresource Project, http://shigen.lab.nig.ac.jp/c.elegans/index.jsp). The *tm2272* allele lacks 626 nucleotides, beginning 80 nucleotides upstream of the predicted EGO-2 translation start side; exons 1–3 are deleted (Figure 3A).

EGO-2 structure: The EGO-2 Bro1 region is located at the amino-terminus of the protein, as is typical for other Bro1-domain proteins (Figure 3, A and B). A Bro1 domain is present in proteins with a variety of functions, including mammalian/yeast Alix/Bro1 endocytic proteins, mammalian nonreceptor protein tyrosine phosphatase, type 23 (HD-PTP), and yeast Rim20, a positive regulator of transcription factor Rim101 activity (Odorizzi 2006). In yeast, the Bro1 region has been shown to be necessary and sufficient for binding a component of *e*ndosomal *s*orting *c*omplex *r*equired for *t*ransport (ESCRT) III and for localization to endosomal compartments (Kim *et al.* 2005).

Many previously described Bro1-domain proteins contain one to two coiled-coil domains downstream of the Bro1 region (see Figure 3C). Coiled-coil domains are protein–protein interaction motifs that are found in a wide range of structural and regulatory proteins (Lupas *et al.* 1991; Mason and Arndt 2004; Rose and Meier 2004). Using the Paircoil prediction program, we detected two putative coiled-coil domains downstream of the Bro1 domain in EGO-2 (Figure 3, B and C).

The C-terminal portion of EGO-2 contains extensive low-complexity sequence and is proline rich. Alix proteins contain several proline-rich protein–protein interaction domains in the C-terminal region (Odorizzi 2006). These specific motifs appear to be absent from EGO-2, but other proline-rich binding motifs may be present. It is intriguing that another *C. elegans* Bro1-domain protein, ALX-1, physically interacts with LIN-12/Notch in the yeast two-hybrid system and has been implicated in its trafficking (Shaye and Greenwald 2005).

Loss of *ego-2* function enhances a weak *glp-1* phenotype in the germline: *ego-2(om33)* was previously identified on the basis of its enhancement of the *glp-1(bn18ts)* germline phenotype at 20° (Qiao *et al.* 1995). After recombining away other mutations on the original *om33* chromosome, we recharacterized the *ego-2(om33)* phenotype. We also characterized the effect of *ego-2(RNAi)* and *ego-2(tm2272)* on *glp-1(ts)* (Table 1; Figure 2). When raised at 20°, 84% of *ego-2(tm2272/om33);glp-1(ts)* animals (obtained from *glp-1(bn18/+)* mothers) had a severe Glp-1 sterile phenotype (Table 1). In these sterile animals, germ cell proliferation failed in early larval development and all germ cells prematurely entered meiosis and differentiated as sperm. Similarly, we observed a Glp-1 sterile defect in 29% of *ego-2(om33); glp-1(bn18)* animals obtained from *ego-2(tm2272/om33); glp-1(bn18/+)* mothers (Table 1, legend). Interestingly, only 8% of adults obtained from an *ego-2(om33); glp-1(bn18ts)* mother were Glp-1 sterile (Table 1), suggesting that there may be a maternal EGO-2 contribution that influences the Ego phenotype. Consistent with these genetic data, 45% of *ego-2(RNAi);glp-1(bn18ts)* adults (on average) were Glp-1 sterile (Table 1). *ego-2(tm2272)* homozygotes did not survive to adulthood, and therefore we could not characterize enhancement of *glp-1(ts)* in this genetic background.

In a *glp-1(+)* background, germline proliferation was maintained in *ego-2(om33)*, *ego-2(om33/tm2272)*, and *ego-2(RNAi)* adult germlines (Table 1; Figure 2). Similarly, germline proliferation was maintained when we performed *ego-2* RNAi in the *rrf-3(0)* genetic background, where RNAi is enhanced (data not shown). RRF-3 is a RNA-directed RNA polymerase (RdRP) whose activity limits the RNAi response; sensitivity to RNAi is

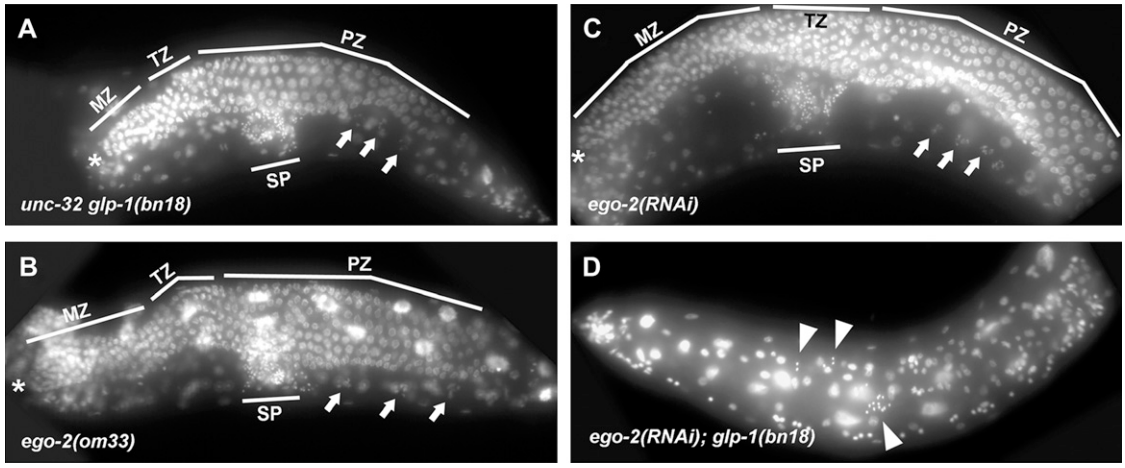

Figure 2.—Enhancement of the *glp-1(ts)* germline phenotype by loss of *ego-2* function. All animals were raised at 20°. An asterisk indicates the distal end of the gonad arm. MZ, mitotic zone; TZ, transition zone (leptotene–zygotene stage); PZ, pachytene zone; sp, sperm; arrows, oocyte; arrowheads in D, sperm. (A) Development of the *glp-1(bn18ts)* adult hermaphrodite germline is normal. Mitotic and meiotic germ cells, developing oocytes, and sperm are present. (B) Mitosis is maintained in *ego-2(om33) unc-75* and (C) *ego-2(RNAi)* germlines. (D) Glp-1 sterile phenotype caused by *ego-2* (Y53H1C.2) RNAi in a *glp-1(bn18ts)* background. In this animal, mitotic proliferation ceased early in larval development and germ cells differentiated as sperm. This phenotype resembles that of *ego-2(om33);glp-1(bn18ts)* sterile hermaphrodites (see Qiao *et al.* 1995).

substantially enhanced in many tissues in the *rrf-3(0)* mutant, including germline (Simmer *et al.* 2002). We conclude that either *ego-2* activity is not absolutely required to maintain germline proliferation or sufficient residual EGO-2 activity remains in our mutants and dsRNA-treated animals to allow proliferation to continue.

Loss of ego-2 function enhances a weak lag-2 phenotype in the gonad: We further investigated the idea that *ego-2* positively regulates the GLP-1 signaling pathway by asking whether *ego-2(RNAi)* could enhance the germline sterile phenotype associated with *lag-2(q420ts)* (Lambie and Kimble 1991). In tests at 15°, ~10% of *lag-2(q420ts)* control animals had a Glp-1 sterile phenotype ($n = 577$ animals, $N = 12$ broods). In contrast, 42% of *lag-2(q420ts); ego-2(RNAi)* animals (on average) had a Glp-1 sterile phenotype ($n = 1119$ animals, $N = 15$ broods). (The percentage of Glp-1 sterility of *lag-2(q420ts); ego-2(RNAi)* animals is the average of two independent RNAi experiments where control and *ego-2(RNAi)* animals were grown in parallel.) We conclude that the loss of *ego-2* function enhances the germline-proliferation-defective phenotype of *lag-2(ts)*.

EGO-2 function in the soma promotes germline proliferation: To investigate whether EGO-2 activity is required in the germline and/or in the soma, we tested the ability of *ego-2(RNAi)* to enhance *glp-1(ts)* in a genetic background where RNAi is disabled in the soma. RRF-1 is an RdRP whose function is required for robust RNAi in the soma; *rrf-1(0)* mutants have a weak response to RNAi in the soma, but normal sensitivity in the germline (Sijen *et al.* 2001). We compared the effect of *ego-2* RNAi in *rrf-1(0);glp-1(bn18ts) vs. rrf-1(+);glp-1(bn18ts)* animals tested in parallel (Table 2). Enhancement of *glp-1* was reduced from ~43% Glp-1 sterility in *ego-2(RNAi);glp-1(bn18ts)* animals to ~14% Glp-1 sterility in *rrf-1(0) ego-2(RNAi);glp-1(bn18ts)* animals. Therefore, EGO-2 activity in the soma is critical for germline proliferation. The weak enhancement observed in the *rrf-1(0); glp-1(ts)* background may reflect residual RNAi in the soma and/or indicate that EGO-2 activity in the germline also (weakly) promotes germline proliferation.

In a complementary approach, we used quantitative reverse transcriptase DNA amplification to examine *ego-2* mRNA expression in the germline *vs.* soma. We compared the *ego-2* mRNA expression level in wild type (N2) *vs. glp-4(bn2ts)* mutant adults raised at restrictive temperature, which have very few germ cells (Beanan and Strom 1992). *ego-2* mRNA was detected with similar intensity in both strains, indicating that expression is not germline specific or germline enriched (data not shown). This result is consistent with our phenotypic data indicating that *ego-2* functions in the soma.

Loss of *ego-2* function enhances *glp-1(ts)* in the embryo: We investigated whether EGO-2 activity positively regulates GLP-1/Notch signaling in other tissues in addition to the gonad. Several inductive events in the embryo are mediated by GLP-1 signaling (Priess 2005). In the early embryo, GLP-1 is maternally provided. Consequently, non-null *glp-1* alleles cause several structural defects in the embryo, resulting in maternal-effect embryonic lethality (a Mel phenotype) (Austin and Kimble 1987; Priess *et al.* 1987). We tested whether *ego-2(om33)* and *ego-2(RNAi)* could enhance the *glp-1(ts)* Mel phenotype. Experimental and control strains were tested in parallel. At 20°, *ego-2(om33)* enhanced the *glp-1(bn18ts)* Mel phenotype from ~15% in *glp-1(bn18)* animals to ~25% in *ego-2(om33); glp-1(bn18)* animals

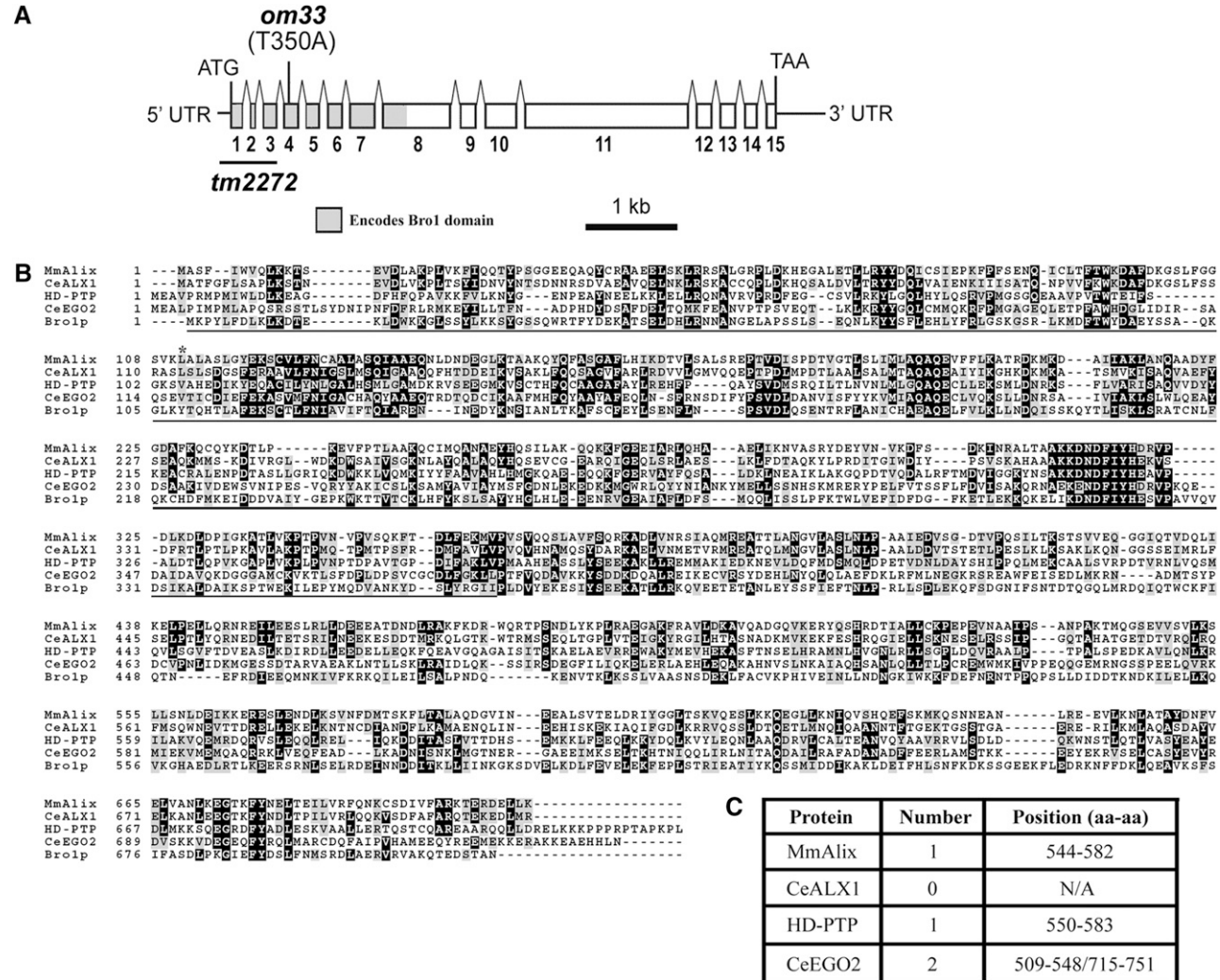

C

Protein	Number	Position (aa-aa)
MmAlix	1	544-582
CeALX1	0	N/A
HD-PTP	1	550-583
CeEGO2	2	509-548/715-751
Bro1p	1	548-583

FIGURE 3.—*ego-2* gene structure. (A) The *ego-2* mRNA structure. Boxes indicate exons. The region encoding the Bro1 domain is shaded; *om33* and *tm2272* lesions are indicated. UTR, untranslated region. (B) Alignment of amino-terminal domains of EGO-2 (CeEGO2), *Mus musculus* Alix (MmAlix; accession no. CAA066329), *C. elegans* ALX-1 (CeALX1; accession no. CAA82667), *Homo sapiens* HD-PTP (accession no. NP_056281), and *Saccharomyces cerevisiae* Bro1 (accession no. P48582). The Bro1 domain is underlined in the alignment. An asterisk indicates the valine residue altered in the *om33* allele. (C) The number of coiled-coil domain(s) in each protein as predicted by Paircoil (probability cutoff: 0.5). The putative coiled-coil domain in ALX-1 reported by SHAYE and GREENWALD (2005) was not identified by the Paircoil program.

(Table 3). In separate assays, *ego-2(RNAi)* enhanced the *glp-1(bn18ts)* Mel phenotype from ~6% in *glp-1(bn18)* animals to ~16% in *glp-1(bn18); ego-2(RNAi)* animals (Table 3). [The *glp-1(bn18)* Mel phenotype is extremely sensitive to temperature, which is why the baseline percentage of Mel value varies from one experiment to another.] To investigate this further, we tested whether *ego-2(om33)* could enhance the Mel-specific allele *glp-1(e2142ts)* (PRIESS *et al.* 1987). At 15°, *glp-1(e2142ts)* mothers produced 0.5% dead embryos; in contrast, *ego-2(om33); glp-1(e2142ts)* mothers produced 14% dead embryos (Table 3). These results suggest that EGO-2 activity promotes (at least in some instances) GLP-1 signaling in the embryo.

To investigate whether the loss of *ego-2* function specifically enhanced the Glp-1 Mel phenotype, we assayed for a specific defect associated with loss of GLP-1 signaling activity. GLP-1 signaling at the four-cell stage ultimately is required for production of the anterior portion of the pharynx; consequently, the posterior bulb of the pharynx forms in Glp-1 Mel embryos but the anterior bulb is absent (PRIESS *et al.* 1987). We examined the dead embryos produced by *ego-2(om33) unc-75;glp-1(ts);nT1 gfp/+* mothers to evaluate their pharynx phenotype. The *nT1 gfp* balancer carries a marker that expresses GFP in the pharynx, allowing us to easily identify pharyngeal cells. Approximately 50% of *ego-2(−); glp-1(bn18ts)* embryos contained a posterior pharynx bulb,

TABLE 2

Enhancement of *glp-1(bn18ts)* by *ego-2(RNAi)* in *rrf-1(0)* background

Genotype	Brood size (*N*)	% Glp-1 sterile progeny (*n*)
ego-2(RNAi)	189 ± 11 (9)	0 (1702)
rrf-1(0) ego-2 (RNAi)	194 ± 5 (8)	0 (1546)
ego-2(RNAi); unc-32 glp-1(bn18ts)	128 ± 3 (17)	43.1 (2189)
rrf-1(0) ego-2(RNAi); unc-32 glp-1(bn18ts)	140 ± 2 (19)	14.4 (2686)

All tests were done at 20°. *N*, number of broods scored; *n*, number of animals scored. "Glp-1 sterile" is as described in the Table 1 legend. Values are the average of three independent sets of RNAi experiments, where each genotype was tested in parallel. Number following the "±" is the standard error of the mean.

TABLE 4

***ego-2(RNAi)* enhances the loss of *lin-12* function in the AC–VU decision**

Genotype	% 2 AC	*n*
lin-12(+)	0	[a]
lin-12(0)	100	[a]
lin-12(ar170); cdh-3::gfp[b]	26	195
ego-2(RNAi); lin-12(ar170); cdh-3::gfp[b]	50	184

All experiments were done at 20°. *n*, total number of animals scored.

[a] Values are from the literature (reviewed by Greenwald 2005).

[b] Data are the average of three independent sets of feeding experiments, where *lin-12(ar170)* was grown in parallel on OP50 and the *ego-2* RNAi bacterial feeding strain. A *Z*-test indicates that *lin-12(ar170); cdh-3::gfp* is significantly different from *ego-2(RNAi); lin-12(ar170); cdh-3::gfp* ($P < 0.05$).

but no anterior one (data not shown). The remaining ~50% of embryos either died too young to evaluate pharyngeal development or, in some cases, developed to the threefold stage and appeared to have both pharyngeal bulbs. We conclude that *ego-2(om33)* and *ego-2(RNAi)* produce a variable phenotype depending on the level of residual EGO-2 activity and that the variability results from defects in one or more different GLP-1-mediated signaling events, overlaid with defects in additional, non-GLP-1-mediated events. These data suggest that EGO-2 function promotes GLP-1/Notch signaling in the embryo; however, additional studies must be done to determine which specific GLP-1/Notch signaling events are affected.

Consistent with our phenotypic results, *in situ* hybridization data from The Nematode Expression Pattern Database reveals expression of *ego-2*/Y53H1C.2 mRNA in the early embryo (http://nematode.lab.nig.ac.jp). At present, postembryonic *in situ* hybridization data are not available.

TABLE 3

***ego-2(om33)* enhances the *glp-1* maternal-effect embryonic lethality**

Temperature	Genotype	Brood size	% dead embryos (*n*)
15°	*glp-1(e2142ts)*	275 ± 10	0.5 (1376)
15°	*ego-2(om33) unc-75*	156 ± 18	0.3 (623)
15°	*ego-2(om33) unc-75; glp-1(e2142ts)*	153 ± 14	14.2 (1831)
20°	*glp-1(bn18ts)*	217 ± 12	9.8 (1083)
20°	*unc-75*	190 ± 10	0.4 (1142)
20°	*ego-2(om33) unc-75*	192 ± 11	0.3 (1152)
20°	*unc-75; glp-1(bn18ts)*	167 ± 4	14.8 (2009)
20°	*ego-2(om33) unc75; glp-1(bn18ts)*	130 ± 15	24.8 (1043)
20°	*unc-36 glp-1(bn18ts)*[a]	171 ± 9	6.3 (1877)
20°	*ego-2(RNAi); unc-36 glp-1(bn18)*[a]	169 ± 7	15.9 (1856)

Number following the "±" is the standard error of the mean. *n*, number of animals scored.

[a] Data are from one RNAi experiment. Additional RNAi experiments were done using a strain with *unc-32* as a marker rather than *unc-36*. The percentage of embryonic lethality was 3.2% in *unc-32 glp-1(bn18)* animals (14 broods, 206 ± 5 animals/brood) and 12.6% in *ego-2(RNAi); unc-32 glp-1(bn18)* (14 broods, 186 ± 6 animals/brood).

Loss of *ego-2* function enhances *lin-12(lf)*: We next examined whether EGO-2 function promotes LIN-12/Notch signaling activity, focusing specifically on the AC–VU decision. During wild-type development, two cells in the larval gonad, Z1.ppp and Z4.aaa, interact via LIN-12-mediated lateral signaling; one cell eventually forms an AC and the other cell forms a VU precursor (Greenwald 2005). LIN-12 activity is required for the VU fate (Greenwald *et al.* 1983). We tested whether *ego-2* activity promotes LIN-12/Notch signaling by testing for enhancement of a weak *lin-12* mutation, *lin-12(ar170)*, in the AC–VU decision. We scored the number of ACs present in L3 stage larvae and used CDH-3::GFP as an AC marker (see materials and methods). CDH-3 is a cadherin that is expressed in a number of epithelial cells; it is expressed at a high level in the newly formed AC (Pettitt *et al.* 1996; Inoue *et al.* 2002). At 20°, we observed two ACs (indicating a failure in LIN-12-mediated signaling) in 26% of *lin-12(ar170)* larvae, similar to reported values (Hubbard *et al.* 1996; see also Chen *et al.* 2004) (Table 4). We consistently observed enhancement of the two-AC defect to 50% in *ego-2(RNAi); lin-12(ar170)* larvae (Table 4). We conclude that EGO-2 activity promotes LIN-12/Notch signaling in the Z1.ppp-Z4.aaa interaction.

We also tested whether *ego-2(RNAi)* altered the AC–VU decision in a *lin-12(+)* background using a *lin-12(+);cdh-3::gfp* strain. All animals observed had only a single AC, suggesting that the effect of *ego-2(RNAi)* on

LIN-12 signaling activity is too mild to produce an effect in this nonsensitized background (data not shown).

Can *ego-2(lf)* suppress hyperactive GLP-1 or LIN-12 activity? To further investigate how EGO-2 activity promotes Notch signaling, we tested whether *glp-1(gf)* or *lin-12(gf)* defects could be suppressed by the loss of *ego-2* function. *glp-1(oz112gf)* causes unregulated germline proliferation, resulting in a tumorous germline (Berry *et al.* 1997). Neither *ego-2(om33)* nor *ego-2(RNAi)* suppressed the *glp-1(oz112)* tumor (data not shown). However, a subtle decrease in tumor size might not be easily observed. Consequently, we tested for suppression of a weaker hypermorphic allele, *glp-1(ar202)*, and suppression of the semidominant *lin-12* allele, *lin-12(n302)* (Greenwald *et al.* 1983). To test for suppression of *lin-12(n302)*, we constructed a *dpy-17 lin-12(n302)/hT2 gfp; cdh-3::gfp* strain and assayed for the presence of an AC in *lin-12(n302/+); ego-2(RNAi)* animals as described above for the *lin-12(ar170)* experiment (see materials and methods). A total of 67% of *lin-12(n302/+)* control animals ($n = 21$) and 64.5% of *ego-2(RNAi); lin-12(n302/+)* animals ($n = 31$) failed to form an AC. To test for suppression of *glp-1(ar202)*, we assayed the proximal proliferation phenotype in L4/young adult hermaphrodites (L1 + 48 hr) raised at 25°. Proximal proliferation was visible in 32% ($n = 62$) of *glp-1(ar202)* controls and 20% ($n = 60$) of *ego-2(RNAi); glp-1(ar202)* animals. Taken together, these data suggest that the loss of *ego-2* function does not suppress a weak *glp-1* or *lin-12* hypermorph.

The relationship between EGO-2 and the meiotic entry pathways: Downstream of GLP-1 signaling, the GLD-1 and GLD-2 pathways act redundantly to promote germ cell entry into meiosis and/or to inhibit continued germ cell proliferation (Hansen and Schedl 2006). Meiotic entry is severely impaired in *gld-2(0) gld-1(0)* double mutants, and germ cells overproliferate to form a tumor (Kadyk and Kimble 1998; Hansen *et al.* 2004). The few germ cells that do enter meiosis never proceed beyond the leptotene–zygotene stage (Hansen *et al.* 2004). We examined the *gld-2(0) gld-1(0) ego-2(om33)* and *gld-2(0) gld-1(0) ego-2(RNAi)* germlines to determine whether a reduction in *ego-2* activity could suppress the *gld-2 gld-1* meiotic entry defect. In both cases, the proportion of leptotene–zygotene germ cells was approximately the same as in the *gld-2 gld-1* control, and pachytene germ cells were not observed (data not shown).

EGO-2 function promotes spermatogenesis: We noted that *ego-2(om33)* animals raised at 25° produced very few progeny (33 ± 5) (Table 5), as did *ego-2(tm2272/om33)* animals at 20° (28 ± 3) (Table 1). In addition, these animals prematurely laid unfertilized oocytes intermittently with fertilized eggs. We monitored these animals and visually inspected them after they had stopped producing embryos. At this point, they retained sperm in the spermatheca (data not shown). Typically, wild-type hermaphrodites do not lay unfertilized oocytes until they are depleted of sperm, and each wild-type sperm will typically fertilize an oocyte. Hence, it appeared that *ego-2(−)* mutants had a Spe defect. Consistent with this, we also noted that the *ego-2(−)* hermaphrodites accumulate endomitotic oocytes in the uterus.

TABLE 5

***ego-2* and *alx-1* promote spermatogenesis**

Genotype	Temperature	Brood size	*N*
Wild-type (N2) hermaphrodite	25°	155 ± 10	10
ego-2(om33) unc-75 hermaphrodite	25°	33 ± 5	10
ego-2(om33) unc-75 hermaphrodite × +/+ male[a]	25°	170 ± 7	12
ego-2(om33) unc-75 hermaphrodite × +/+ male[b]	25°	119 ± 5	5
unc-75 hermaphrodite × +/+ male[b]	25°	177 ± 14	7
unc-75; alx-1(0) hermaphrodite	25°	124 ± 8	11
ego-2(om33) unc-75; alx-1(0) hermaphrodite	25°	6 ± 1	10
ego-2(om33) unc-75; alx-1(0) hermaphrodite × +/+ male[b]	25°	117 ± 6	10
ego-2(tm2272/om33) male × *fog-1(ts)* female[c,d]	25°	<1 ± 1	25
+ male × *fog-1(ts)* female[c]	25°	71 ± 4	10

N, total number of broods scored. Number following the "±" is the standard error of the mean. Broods were assayed on consecutive days, until at least 1 day after hermaphrodites had stopped producing embryos. At this point, visual examination revealed the presence of (apparently nonfunctional) sperm in *ego-2(om33) unc-75* and *ego-2 unc75; alx-1* hermaphrodites and in the mating partners of *ego-2(tm2272/om33)* males.

[a] Two males mated with each hermaphrodite.

[b] Three males mated with each hermaphrodite.

[c] Five males mated with each hermaphrodite. *unc-75*-marked hermaphrodites consistently fared better when mated with fewer males.

[d] Only four matings produced progeny (one to five per mother).

To confirm that the small brood sizes result from a defect in sperm rather than an oocyte function, we asked if the *ego-2* hermaphrodite brood size could be increased by mating with wild-type (N2) males (see materials and methods). Upon mating at 25°, brood sizes of *ego-2(om33) unc-75* hermaphrodites increased substantially, indicating that the oocytes were functional and could be fertilized by wild-type sperm (Table 5). We conclude that the *ego-2(om33)* hermaphrodites (at 25°) have an incompletely penetrant sperm defect.

To investigate whether *ego-2* promotes spermatogenesis in males, we generated *ego-2(tm2272/om33)* males and mated them with *fog-1(q352ts)* females raised at 25° (see materials and methods). When wild-type (N2) males were mated with *fog-1(ts)* females at 25°, 10/10 matings produced progeny (Table 5). In contrast, when *ego-1(tm2272/om33)* males were mated with *fog-1(ts)* females, only 4/25 matings produced progeny, and

the number of progeny was extremely small (Table 5). Visual inspection indicated that *ego-2(tm2272/om33)* males produced substantial numbers of sperm, and the mated *fog-2(ts)* females contained sperm, indicating that sperm had been transferred (data not shown). On the basis of these data, we conclude that *ego-2(tm2272/om33)* males produce defective sperm.

Additional *ego-2* functions: A variety of defects were observed in the somatic tissues of *ego-2(tm2272)* and *ego-2(RNAi); rrf-3(0)* animals, at least some of which are in processes not known to involve Notch signaling. The *ego-2(tm2272)* allele is associated with developmental arrest/lethality of embryos/young larvae. We did not observe significant levels of embryonic or early larval lethality when *ego-2* RNAi was performed in the *ego-2(om33)* mutant background or in the *rrf-3(0)* enhanced RNAi background. However, *ego-2(RNAi)* animals developed slowly, reaching adulthood ~24 hr later than controls; they were also uncoordinated (data not shown). *ego-2(RNAi)* adults had an egg-laying (Egl) defect, perhaps reflecting a vulval defect. Taken together, these phenotypic data indicate that EGO-2 activity is important for multiple aspects of development.

We were concerned that *ego-2(RNAi)* did not phenocopy the lethality that is associated with *tm2272* and considered that the lethality might arise from a second linked mutation alone or in combination with *tm2272*. To examine this issue, we evaluated the phenotypes of *ego-2(tm2272)/hDf17* and *ego-2(om33)/hDf17* animals (see MATERIALS AND METHODS). *hDf17* uncovers the *ego-2* gene region (see http://www.wormbase.org). *ego-2(om33)/hDf17* hermaphrodites are Spe and resemble *ego-2(om33/tm2272)* animals (data not shown). This result suggests that *tm2272* behaves like *hDf17* and is null for *ego-2* function. In contrast, we were not able to recover *ego-2(tm2272)/hDf17* adults, suggesting that this genotype is lethal (see MATERIALS AND METHODS). Alternatively, *hDf17* might uncover a second linked mutation that causes the lethality. To try to resolve this question, we generated an *ego-2(+)* construct and used it to generate multicopy extrachromosomal transgenic arrays. Two different transgenic arrays, *omEx35* and *omEx36*, were crossed into the *ego-2(tm2272/+)* background, and *ego-2(tm2272);omEx35* and *ego-2(tm2272);omEx36* adult hermaphrodites were recovered (Y. LIU and E. MAINE, unpublished data). Therefore, the *ego-2(+)* transgenic arrays apparently rescued the early larval lethality, indicating that the lethality is associated with the *tm2272* deletion. A formal possibility remains, however, that this is a synthetic lethality caused by *tm2272* and a second linked mutation (uncovered by *hDf17*).

***ego-2* and *alx-1* interact genetically:** SHAYE and GREENWALD (2005) have previously shown that ALX-1 physically interacts with LIN-12/Notch in the yeast two-hybrid system and acts as a negative regulator of LIN-12 activity. During vulva formation, LIN-12 is downregulated in the vulval precursor cell (VPC) that takes on the primary fate, typically P6.p; ALX-1 activity is required for LIN-12 degradation after internalization in the 1° VPC (SHAYE and GREENWALD 2005). On the basis of their analysis of ALX-1 localization and its molecular structure, SHAYE and GREENWALD (2005) propose that ALX-1 associates with the multivesicular endosome. We investigated whether ALX-1 activity promotes GLP-1/Notch signaling and the functional relationship between ALX-1 and EGO-2.

TABLE 6

***alx-1(0)* suppresses the enhancement of *glp-1(ts)* by *ego-2* in the germline**

Genotype	Brood size (*N*)	% Glp-1 sterile (*n*)
ego-2(RNAi)	192 ± 6 (3)	0 (575)
alx-1(0)	234 ± 6 (19)	0.1 (4453)
unc-36 glp-1(bn18)	171 ± 9 (11)	1.0 (1877)
unc-36 glp-1(bn18) alx-1(0)	178 ± 7 (10)	0.1 (1783)
ego-2(RNAi); alx-1(0)	186 ± 3 (6)	0 (1114)
ego-2(RNAi); unc-36 glp-1(bn18)[a]	168 ± 7 (11)	27 (1856)
ego-2(RNAi); unc-36 glp-1(bn18) alx-1(0)[a]	177 ± 8 (8)	11 (1413)

All tests were done at 20°. "Glp-1 sterile" is as described in the Table 1 legend. *N*, number of broods scored; *n*, number of animals scored.

[a]Two independent RNAi experiments were done. We consistently observed reduced enhancement of *glp-1* in *alx-1(0) vs. alx-1(+)* animals.

To examine these questions, we first constructed a *glp-1(bn18ts) alx-1(0)* double mutant and tested for enhancement of *glp-1(ts)* in the germline at 20°. We did not observe enhancement (Table 6). Next, we tested whether *alx-1* might potentiate the enhancement of *glp-1* by *ego-2*. Surprisingly, the Glp-1 phenotype was *less* pronounced in *ego-2(RNAi);glp-1(bn18ts) alx-1(0)* germlines compared with the *ego-2(RNAi); glp-1(bn18ts)* germlines (Table 6). This result suggested that EGO-2 and ALX-1 may have opposite functions with respect to GLP-1 pathway activity, at least in the germline. Alternatively, *alx-1(0)* mutants may have reduced sensitivity to RNAi. To test this possibility, we constructed an *alx-1(0)* strain that carried a *gfp*-tagged transgene (*ccIs4251*) and performed RNAi, targeting the *gfp* mRNA for degradation (see MATERIALS AND METHODS). GFP expression was reduced to below visible levels in both *alx-1(+)* and *alx-1(0)* strains upon *gfp* RNAi (data not shown). Hence, *alx-1(0)* mutants are sensitive to RNAi.

We also examined the phenotype of *ego-2(lf);alx-1(0)* animals in a *glp-1(+)* background. At 25°, the *ego-2(om33); alx-1(0)* double mutant had a brood size of 6 ± 1, which is substantially smaller than the *ego-2(om33)* single mutant (Table 5). Visual inspection indicated that these animals retained a population of mitotic germ cells and were actively making oocytes; they also retained

significant stores of sperm, which apparently could not fertilize the oocytes. Consistent with this conclusion, endomitotic oocytes were present in the uterus (but not in the oviduct). To confirm that the sperm were defective, we mated *ego-2(om33) unc-75; alx-1(0)* hermaphrodites with wild-type (N2) males at 25° and assayed their brood sizes (see MATERIALS AND METHODS). The average brood size increased substantially (Table 5), indicating that the *ego-2(om33);alx-1(0)* oocytes can be fertilized by wild-type sperm. We conclude that most *ego-2(om33);alx-1(0)* self-sperm were defective. As we observed for unmated *ego-2;alx-1* double mutants, visual examination of mated *ego-2(om33);alx-1(0)* hermaphrodites revealed that their germline retained a distal mitotic population and were actively producing oocytes. We conclude that *alx-1(0)* interacts synergistically with *ego-2(om33)* to cause a more highly penetrant spermatogenesis defect than is produced by *ego-2(om33)* alone.

DISCUSSION

ego-2 was previously identified as a positive regulator of germline proliferation that interacts genetically with *glp-1* (QIAO *et al.* 1995). Here, we have characterized the *ego-2* gene structure and shown that its conceptual translation product is a Bro1-domain protein. We demonstrated that the loss of EGO-2 function impairs signaling via GLP-1/Notch in the germline and embryo and via LIN-12/Notch in the AC–VU decision. We also demonstrate that the loss of EGO-2 function impairs signaling via LAG-2, the predominant DSL-type ligand known to act in the DTC and in the AC–VU precursors. In the embryo, EGO-2 activity presumably promotes activity via additional ligands, *e.g.*, APX-1. Additional experiments will be required to determine whether EGO-2 is a universal promoter of Notch-type signaling in all tissues.

Our data indicate that EGO-2 activity in the soma positively regulates germline proliferation in the sensitized *glp-1(ts)* background. We hypothesize that it is specifically EGO-2 expression in the somatic gonad that promotes GLP-1 signaling in the germline, although additional expression data will be required to confirm this hypothesis. In addition, our data also suggest that EGO-2 activity in the germline itself positively regulates proliferation.

The relationship between EGO-2 and ALX-1: Our genetic data suggest a complex functional relationship between EGO-2 and the related Bro1-domain protein, ALX-1. The two proteins appear to act in opposition with respect to some processes (*e.g.*, GLP-1/Notch signaling in the gonad) and in concert with respect to other ones (*e.g.*, spermatogenesis). ALX-1 activity has been shown to promote downregulation of internalized LIN-12::GFP in the 1° VPC during vulval development, and GFP::ALX-1 was shown to localize to subcellular foci that are suggestive of endosomal compartments (SHAYE and GREENWALD 2005). More recently, GFP::ALX-1 was shown to colocalize with integral endosomal components (B. GRANT, personal communication), strengthening the hypothesis that ALX-1 regulates LIN-12 trafficking. Although *alx-1(RNAi)* did not mimic a *lin-12* mutant phenotype in the vulval precursor cell interaction (SHAYE and GREENWALD 2005), it remains to be shown whether *alx-1(0)* can enhance or suppress the *lin-12(−)* phenotype in certain tissues. Given the observations of SHAYE and GREENWALD (2005) and the data reported here, we hypothesize that ALX-1 may be a negative regulator of GLP-1 activity in the germline.

EGO-2 functions in events not known to require Notch activity: EGO-2 activity also promotes aspects of somatic and germline development that have not yet been linked to Notch signaling. We speculate that EGO-2 functions in the trafficking or regulation of additional cell-surface proteins whose activities promote these other aspects of development. In spermatogenesis, for example, EGO-2 may function in endocytic events that regulate a number of different events, *e.g.*, biogenesis of the membraneous organelle or its function during spermiogenesis or trafficking/activation of cell-surface proteins that mediate sperm–egg binding (reviewed by L'HERNAULT 2006).

EGO-2 may function in endocytic processes that promote Notch signaling: Bro1-domain proteins have been implicated in a variety of cellular processes in fungi, plants, and animals. Several Bro1-domain proteins, as well as the isolated Bro1 domain itself, have been shown to localize to late endosomes and contain a binding motif for a specific subunit of ESCRT-III (KIM *et al.* 2005). ESCRT-I, -II, and -III are protein complexes that function in trafficking (mono-ubiquitinated) transmembrane proteins to multivesicular bodies. Although we have not demonstrated here that EGO-2 localizes to endosomes, this hypothesis is strengthened by the observation that ALX-1 does so (B. GRANT, personal communication).

Classically, endocytosis has been understood to function in the negative regulation of signal transduction, *e.g.*, by removal of spent receptor from the plasma membrane. More recently, endocytosis has been shown to promote signal transduction in many situations, although the mechanisms by which this occurs are not clear (MAXFIELD and MCGRAW 2004; MIACZYNSKA *et al.* 2004). Studies in several organisms have shown that Notch-type signaling is subject to both positive and negative regulation via endocytosis (LE BORGNE *et al.* 2005; WILKIN and BARON 2005; CHITNIS 2006). In *C. elegans*, endocytic processes have been implicated in the positive regulation of Notch signaling in the gonad, where inactivation of epsin in the somatic gonad has been shown to enhance the phenotype of a weak *glp-1* loss-of-function mutation in the germline (TIAN *et al.* 2004).

Various models have been proposed for how endocytosis might promote Notch-type signaling (see MIACZYNSKA

et al. 2004; Le Borgne *et al.* 2005; Chitnis 2006; Le Borgne 2006; Nichols *et al.* 2007). It has been posited that, in the signaling cell, endosomal trafficking may be required for activation or secretion of ligand and that endocytosis of ligand following its interaction with Notch is required for subsequent cleavage of Notch. In the receiving cell, activation of signaling components similarly may be mediated via endocytosis, and/or the final (S3) cleavage event may occur within endocytic vesicles (Gupta-Rossi *et al.* 2004). Since EGO-2 has a Bro1 domain and Bro1-domain proteins have been implicated in endosomal trafficking, we speculate that EGO-2 functions in one or more such endosomal process(es) to promote Notch-type signaling in *C. elegans*. Investigation of the EGO-2 localization pattern and the effect of *ego-2* mutations on endosomal trafficking will help to resolve these issues. Moreover, it will be of interest to investigate whether Bro1-domain proteins regulate Notch-type signaling in other species.

We thank Valarie Vought, Barth Grant, Jane Hubbard, Barbara Conradt, Dave Hansen, Tim Schedl, Aaron Mitchell, Steve L'Hernault, and Xingyu She for fruitful discussions during the course of this work and two anonymous reviewers for comments on the manuscript. We acknowledge Anne Smardon, Li Qiao, Deb Swenton, and Kathryn Mikalak for their participation in the early phases of the *ego-2* study. We thank Yuji Kohara and colleagues for yk1162g08, Shohei Mitani and colleagues for *tm2272*, and Xingyu She for assistance with the figures. Some of the strains used in this study were provided by the Caenorhabditis Genetics Center, which is supported by the National Institutes of Health National Center for Research Resources. Funding was provided by the National Science Foundation and Syracuse University.

LITERATURE CITED

Austin, J., and J. Kimble, 1987 *glp-1* is required in the germ line for regulation of the decision between mitosis and meiosis in *C. elegans*. Cell **51:** 589–599.

Beanan, M. J., and S. Strome, 1992 Characterization of a germline proliferation mutation in *C. elegans*. Development **116:** 755–766.

Berry, L. W., B. Westlund and T. Schedl, 1997 Germline tumor formation caused by activation of *glp-1*, a member of the *Notch* family of receptors. Development **124:** 925–936.

Chen, C. K., K. Bradnam, R. Durbin and J. Hodgkin, 2003 *Genetic Map of Caenorhabditis elegans*. Caenorhabditis Genetics Center, St. Paul.

Chen, J., X. Li and I. Greenwald, 2004 *sel-7*, a positive regulator of *lin-12* activity, encodes a novel nuclear protein in *Caenorhabditis elegans*. Genetics **166:** 151–160.

Chitnis, A. B., 2006 Why is Delta endocytosis required for effective activation of Notch? Dev. Dyn. **235:** 886–894.

Ehebauer, M., P. Hayward and A. Martinez-Arias, 2006 Notch signaling pathway. Sci. STKE **314:** 1414–1415.

Epstein, H. F., and D. C. Shakes, 1995 *Caenorhabiditis elegans: Biological Analysis of an Organism* (Methods in Cell Biology, Vol. 48). Academic Press, San Diego.

Greenwald, I., 2005 LIN-12/Notch signaling in *C. elegans* (August 4, 2005), in *WormBook*, edited by The *C. elegans* Research Community (http://www.wormbook.org).

Greenwald, I. S., P. W. Sternberg and H. R. Horvitz, 1983 The *lin-12* locus specifies cell fates in *Caenorhabditis elegans*. Cell **34:** 435–444.

Gupta-Rossi, N., E. Six, O. LeBail, F. Logeat, P. Chastagner *et al.*, 2004 Monoubiquitination and endocytosis direct gamma-secretase cleavage of activated Notch receptor. J. Cell Biol. **166:** 200473–200483.

Hansen, D., and T. Schedl, 2006 The regulatory network controlling the proliferation-meiotic decision in the *Caenorhabditis elegans* germ line. Curr. Top. Dev. Biol. **76:** 185–215.

Hansen, D., E. J. A. Hubbard and T. Schedl, 2004 Multi-pathway control of the proliferation versus meiotic development decision in the *Caenorhabiditis elegans* germ line. Dev. Biol. **268:** 342–357.

Hubbard, E. J., O. Dong and I. Greenwald, 1996 Evidence for physical and functional association between EMB-5 and LIN-12 in *Caenorhabditis elegans*. Science **273:** 112–115.

Inoue, T., D. R. Sherwood, G. Aspock, J. A. Butler, B. P. Gupta *et al.*, 2002 Gene expression markers for *Caenorhabditis elegans* vulval cells. Gene Expr. Patterns **2:** 235–241.

Kadyk, L. C., and J. Kimble, 1998 Genetic regulation of entry into meiosis in *Caenorhabditis elegans*. Development **125:** 1803–1813.

Kim, J., S. Sitaraman, A. Hierro, B. M. Beach, G. Odorizzi *et al.*, 2005 Structural basis for endosomal targeting by the Bro1 domain. Dev. Cell **8:** 937–947.

Kimble, J., and S. L. Crittenden, 2005 Germline proliferation and its control (August 15, 2005), in *WormBook*, edited by The *C. elegans* Research Community (http://www.wormbook.org).

Lambie, E. J., and J. Kimble, 1991 Two homologous regulatory genes, *lin-12* and *glp-1*, have overlapping functions. Development **112:** 231–240.

Le Borgne, R., 2006 Regulation of Notch signaling by endocytosis and endosomal sorting. Curr. Opin. Cell Biol. **18:** 213–222.

Le Borgne, R., A. Bardin and F. Schweisguth, 2005 The roles of receptor and ligand endocytosis in regulating Notch signaling. Development **132:** 1751–1762.

L'Hernault, S. W., 2006 Spermatogenesis (February 20, 2006), in *WormBook*, edited by The *C. elegans* Research Community (http://www.wormbook.org).

Lupas, A., M. Van Dyke and J. Stock, 1991 Predicting coiled coils from protein sequences. Science **252:** 1162–1164.

Maine, E. M., D. Hansen, D. Springer and V. E. Vought, 2004 *Caenorhabditis elegans atx-2* promotes germline proliferation and the oocyte fate. Genetics **168:** 817–830.

Mason, J. M., and K. M. Arndt, 2004 Coiled coil domains: stability, specificity, and biological implications. Chem. Biochem. **5:** 170–176.

Maxfield, F. R., and T. E. McGraw, 2004 Endocytic recycling. Nat. Rev. Mol. Cell Biol. **5:** 121–132.

Miaczynska, M., L. Pelkmans and M. Zerial, 2004 Not just a sink: endosomes in control of signal transduction. Curr. Opin. Cell Biol. **16:** 400–406.

Nichols, J. T., A. Miyamoto, S. L. Olsen, B. D'Souza, C. Yao *et al.*, 2007 DSL ligand endocytosis physically dissociates Notch1 heterodimers before activating proteolysis can occur. J. Cell Biol. **176:** 445–458.

Odorizzi, G., 2006 The multiple personalities of Alix. J. Cell Sci. **119:** 3025–3032.

Pettitt, J., W. B. Wood and R. H. Plasterk, 1996 *cdh-3*, a gene encoding a member of the cadherin superfamily, functions in epithelial cell morphogenesis in *Caenorhabditis elegans*. Development **122:** 4149–4157.

Priess, J., 2005 Notch signaling in the *C. elegans* embryo (June 25, 2005), in *WormBook*, edited by The *C. elegans* Research Community (http://www.wormbook.org).

Priess, J. R., H. Schnabel and R. Schnabel, 1987 The *glp-1* locus and cellular interactions in early *C. elegans* embryos. Cell **51:** 601–611.

Qiao, L., J. L. Lissemore, P. Shu, A. Smardon, M. Gelber *et al.*, 1995 Enhancers of *glp-1*, a gene required for cell-signaling in *Caenorhabditis elegans*, define a set of genes required for germline development. Genetics **141:** 551–569.

Rose, A., and I. Meier, 2004 Scaffolds, levers, rods and springs: diverse cellular functions of long coiled-coil proteins. Cell. Mol. Life. Sci. **61:** 1996–2009.

Rual, J. F., J. Ceron, J. Koreth, T. Hao, A. S. Nicot *et al.*, 2004 Toward improving *Caenorhabditis elegans* phenome mapping with an ORFeome-based RNAi library. Genome Res. **14:** 2162–2168.

Schweisguth, F., 2004 Notch signaling activity. Curr. Biol. **14:** R129–R138.

Shaye, D. D., and I. Greenwald, 2005 LIN-12/Notch trafficking and regulation of DSL ligand activity during vulval induction in *Caenorhabditis elegans*. Development **132:** 5081–5092.

Sijen, T., J. Fleenor, F. Simmer, K. L. Thijssen, S. Parrish *et al.*, 2001 On the role of RNA amplification in dsRNA-triggered gene silencing. Cell **107:** 465–476.

Simmer, F., M. Tijsterman, S. Parrish, S. P. Koushika, M. L. Nonet *et al.*, 2002 Loss of the putative RNA-directed RNA polymerase RRF-3 makes *C. elegans* hypersensitive to RNAi. Curr. Biol. **12:** 1317–1319.

Sun, A. Y., and E. J. Lambie, 1997 *gon-2*, a gene required for gonadogenesis in *Caenorhabditis elegans*. Genetics **147:** 1077–1089.

Tian, X., D. Hansen, T. Schedl and J. B. Skeath, 2004 Epsin potentiates Notch pathway activity in *Drosophila* and *C. elegans*. Development **131:** 5807–5815.

Timmons, L., D. L. Court and A. Fire, 2001 Ingestion of bacterially expressed dsRNAs can produce specific and potent genetic interference in *Caenorhabditis elegans*. Gene **263:** 103–112.

Weinmaster, G., and R. Kopan, 2006 A garden of Notch-ly delights. Development **133:** 3277–3282.

Wilkin, M. B., and M. Baron, 2005 Endocytic regulation of Notch activation and down- regulation. Mol. Membr. Biol. **22:** 279–289.

Wilson, A., and F. Radtke, 2006 Multiple functions of Notch signaling in self-renewing organs and cancer. FEBS Lett. **580:** 2860–2868.

Communicating editor: D. I. Greenstein